Storage of energy using a Gas-Liquid H_2/Cl_2 fuel cell: a first approach to electrochemically-assisted absorbers

M. Carvela, J. Lobato, M.A. Rodrigo*

University of Castilla-La Mancha, Faculty of Chemical Sciences & Technologies, Chemical Engineering Department, Av. Camilo José Cela, 12. 13071. Ciudad Real, Spain.

Abstract

In this work, the use in fuel cell mode of three electro-absorbers is evaluated for the chloralkaline process and performance is compared with that of a conventional PEMFC operated at the same operation conditions (room temperature). To do this, four cells have been in-house manufactured and compared, in order to determine which electrolyte (solution containing the active species or the membrane) is the best and which is the influence of the absorption stage on the operation of the cell. Because of the high solubility of chlorine, only the hydrogen absorption has been considered in order to evaluate relevant differences in the performance. Results demonstrate that design of the cell has a superb significance on the performances obtained. Cells with membrane-electrode assemblies are more efficient than those in which the membrane is used only as an electrodic compartment separator and utilization of devices which produce tiny bubbles of gas into the electrolyte is also very advantageous in order to obtain higher efficiencies. Results are of a great significance for the design of electro-absorbers and this paper is a first approach to face the design of reversible electrochemical cells for the chloralkaline process.

Keywords

Chloralkaline; fuel cells; microbubbles; electro-absorber; membrane-electrode assembly

Highlights

- Chloralkaline fuel cells can be operated with different types of electro-absorbers
- Size of hydrogen bubbles fed to the cell has a great influence on the performance
- Cells based on MEAs are more efficient than those with separated electrodes
- Maximum production of electricity at room temperature is 6.1 mW cm^{-2}
- Maximum efficiency at room temperature is 50 mWh g^{-1} H_2

*author to whom all correspondence should be addressed: manuel.rodrigo@uclm.es

Introduction

Design of electrochemical cells is a topic of the major interest for the development of sustainable processes (Bebelis et al., 2013). In fact, the design of this type of reactors is, perhaps, one of the most exciting projects that a Chemical Engineer can face, because of the great influence that many of the design parameters can have on the resulting electrochemical reaction performance.

One of the important aspects which needs for further development in electrochemical cells technology is the processing of gases, with many interesting applications in environmental remediation and in energy storage. In an electrochemical cell, there are always two circuits: one electric, that transport electrons from the anode to the cathode, and one ionic, which balances electroneutrality in the cell by transporting anions and cations inside the electrolyte. Both are necessary and efficient operation in terms of energy consumption (or production) would rely on a proper choice of the electrolyte for a given application. Obviously, a gas cannot be an electrolyte, because it cannot transport ions, so to properly manage gases in electrochemical cells there are two possibilities: the conventional use of a solid electrolyte in intimate contact with the electrodes and the absorption of the reactive species of the gas into a liquid electrolyte.

The first approach is used in the conventional Proton Exchange Membranes (PEM) and Solid Oxide (SO) fuel cells, either with a polymer exchange membrane or a solid ceramic electrolyte, respectively. In this approach, the gaseous reagents interact directly with the electrodes without the necessity of a liquid electrolyte, because the ionic circuit is closed with the contact of the two electrodes with the solid electrolyte in which ions are transported. The second approach is applied in many other different processes, such as the production of hydrogen peroxide or ozone from the cathodic or anodic reaction of oxygen (Fernando Perez et al., 2019; Perez et al., 2019), respectively, or the electro-

scrubbing for the removal of VOCs and other environmental pollutants(Yang et al., 2011; Balaji et al., 2015; Govindan and Moon, 2015). It is more complex, because the electrolyte is the liquid in which the gas is dissolved and the initial stage of dissolution of the gas into the electrolyte is very important in order to achieve high reagent concentrations, which help to avoid mass transport limitations in the electrochemical process. This means that the physical absorption and the electrochemical reaction are really integrated in one unit, which can be considered either as an electro-absorber (electrochemically assisted absorption unit) or as a gas-liquid electrochemical cell, because both unit operations (absorption and reaction) are equally important for the success of the technology.

Regarding the application of electrochemical cells to transform fuels into electricity, both cells approaches can be used when processing gases. At high temperatures (above water boiling point) only SOFC approach and PEMFCs equipped with PBI (or similar) membranes can be used (Lobato et al., 2007). At low temperatures (below water boiling point), conventional PEM cells and gas-liquid electrochemical cells (electro-absorbers) can compete, and it is interesting to compare them. Thus, both approaches have advantages and drawbacks. Management of water produced at low temperatures in PEMFC fed with gases is one of their main drawbacks, as well as the necessity of developing electrodes capable to produce an efficient contact between the membrane, the catalyst of the electrodes and the gas stream (Verhage et al., 2013). Technology related to MEAs (Membrane Electrode Assemblies) has been improved for decades and, now, it is at a mature state, although in continuous progress, especially in terms of durability of the systems developed. Channels for a proper distribution of the gas inside the MEAs, and a careful selection of operation conditions, are also required for a successful operation of this technology.

On the other hand, despite being conceptually easier, combination of gas-liquid absorption and electrochemical processes is not as well developed, and there are still many flanks for being competitive(Pillai et al., 2009; Adam Gopal et al., 2018). A proper choice of the formulation of the electrolyte may promote

1) lower electric resistances in the electrochemical cell, associated to a higher ionic conductivity, and/or
2) higher solubilities of the reagents contained in the gases into the liquid, associated to the interactions of the species of the gas which aim to be transported into the liquid with species contained in this liquid phase.

In addition, the selection of operation conditions in the absorption process is very important, in particular to promote dissolution of the gas into the electrolyte when the reagent transferred is consumed on the electrodes. Thus, as an example of the complex interactions expected in these systems, the heat produced during operation of electrochemical cells (by ohmic loses) disfavors the solubility of gases into the electrolyte and makes the overall process less efficient.

Within the energy storage applications, recently, the use of chloralkaline technology has been proposed as a very interesting alternative (Thomassen et al., 2006a; Thomassen et al., 2006b; Thomassen et al., 2006c; Bechtel et al., 2018), with great perspectives in the optimized management of green energy. Thus, to properly manage the energy produced in wind turbines or solar photovoltaic panels, one of the most promising technologies consists of the transformation of water into oxygen and hydrogen by electrolysis using the surplus energy produced with these renewable technologies (eqs. 1 and 2). These reagents can be stored (in fact, only the hydrogen) and used later in a fuel cell to produce electricity when needed.

$$H_2O \rightarrow 0.5\ O_2 + 2H^+ + 2e^- \quad (1)$$

$$2\ H_2O + 2e^- \rightarrow H_2 + 2\ OH^- \quad (2)$$

120 The chloralkaline alternative consists of oxidizing a brackish solution containing sodium
121 chloride, forming chlorine (eq. 3) instead of oxygen and hydrogen (eq. 2), using the well-
122 known electrolytic technology with Mixed Metal Oxides (MMO) electrodes. For
123 hydrogen evolution, platinum-based electrodes are used, which are known for their high
124 efficiency in the oxidation reaction of hydrogen to protons. Instead, for chlorine
125 evolution, MMO electrodes based on ruthenium oxides are used, which is widely used in
126 the oxidation reaction of chlorides to chlorine.

127 $2Cl^- \rightarrow Cl_2 + 2e^-$ (3)

128 Both products can be stored and when needed, they can produce again electricity using a
129 fuel cell fed with chlorine instead of oxygen as oxidant.
130 As it is well-known, chlorine is a much stronger oxidant and it is expected a better
131 performance in fuel cells(Thomassen et al., 2006c), once all the weaknesses foreseeable
132 for this technology could be overcome. In this case, the development of reversible
133 electrochemical cells could be of a great interest, considering that the electrolyzer mode
134 can only work efficiently with liquid streams as, despite there are works in which gaseous
135 HCl is fed(Bechtel et al., 2018), the efficiency obtained is much lower. Our group has
136 started to work in this technology recently and we have realized that the design of the
137 cells is a very important aspect, with many aspects that needs for additional studies.
138 Taking into account this background, this work is going to be focused not on the complete
139 energy storage system, but only on the evaluation of different electrochemical cell
140 prototypes for reaching an efficient H_2/Cl_2 fuel cell operation. It is a first stage in a more
141 ambitious project, in which later these prototypes aim to be integrated into a reversible
142 electrochemical cell concept for the chloralkaline process. Two main types of cells are
143 used to evaluate the four prototypes (Figure 1):

1) a divided cell in which the membrane function is only to separate the anionic and cationic compartments and in which the electrode gap is wide (1 cm) (used in prototypes 1 and 2) and

2) a PEM cell in which the membrane act as the electrolyte (prototypes 3 and 4).

In the four systems, a hypochlorite solution is fed to the cathode. Opposite, hydrogen is fed to the anode after absorption in a 2.0M NaCl electrolyte solution by means of a conventional jet mixer (prototype 1) or a mechanical device developed to produce microbubbles (prototypes 2 and 3), based on the sudden change of pressure from 3 to 1 bars. Results obtained with these three prototypes will be compared to those obtained by Prototype 4, in which hydrogen is added as a gas with no previous absorption stage into a liquid electrolyte. The aim is to evaluate if the use of the hydrogen fuel dissolved in a liquid can improve the performance of the fuel cell.

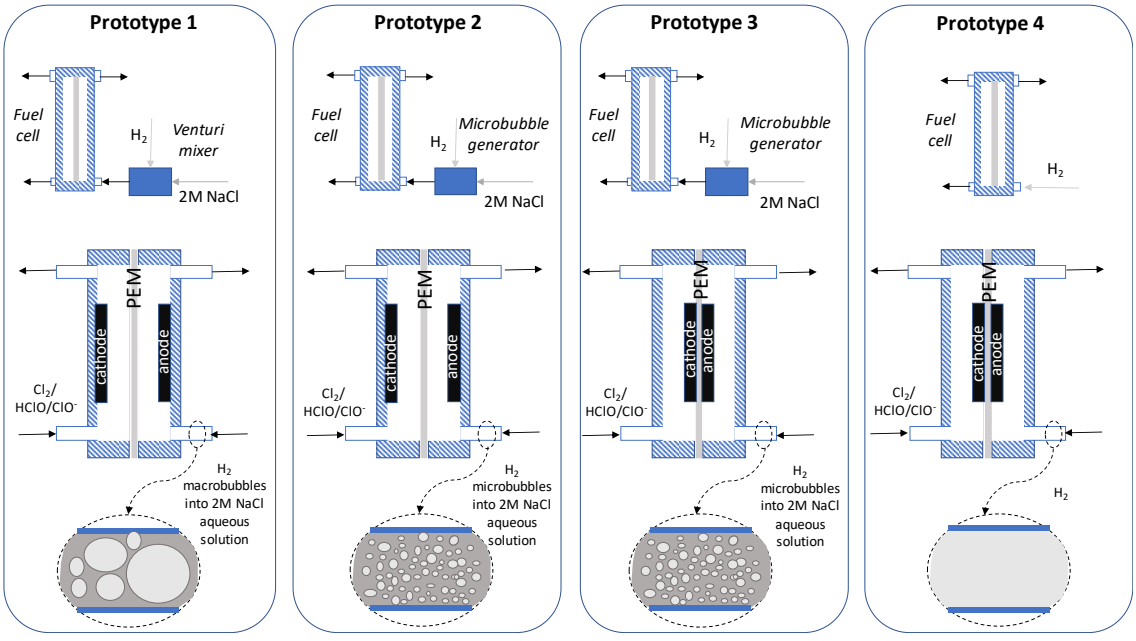

Figure 1. Layout of the four prototypes aimed to be studied in this work

Materials and Methods

Electrodes preparation. Two types of electrodes were prepared depending on the type of cell. For the cells in which no MEA was used, the electrodes consist of mixed metal oxides (MMO) coatings prepared on titanium plates (2.0x1.0x0.1 cm^3) used as electrode support. Plates were chemically pre-treated, first in hot hydrochloric acid 20% (w/w) for 15 minutes and, then, in hot oxalic acid 10% (w/w) for other 15 minutes. Finally, the supports were washed with Milli-Q water (resistivity ≥18.2 MΩ cm at 25 °C). The Pechini Method was followed (Freitas et al., 2006a; Freitas et al., 2006b). Thus, the metallic precursors are dissolved at 60ºC in an ethylene glycol (EG) solution (Merck, 99.0% v/v). the citric acid, CA, (Sigma, 99.5% w/w) is added, with EG/CA/metallic precursors molar ratio of 10:3:1.

For the cathode (electrode in charge of the electrochemistry of chlorine), $RuCl_3 \cdot 3H_2O$ (Alfa Aesar, Ru 38% w/w), $C_{16}H_{36}O_4Ti$ (Sigma-Aldrich, 97% v/v) and $H_2PtCl_6 \cdot 7H_2O$ (Merck, Pt 40% w/w) were used are precursor in suitable amounts into this solution in order to manufacture a $Ti/Ru_{0.3}\,Ti_{0.6}\,Pt_{0.1}$ electrode.

For the anode (electrode in charge of the hydrogen electrochemistry), no ruthenium salts were used, and the ratio used was to obtain a formulation $Ti_{0.8}Pt_{0.2}$. The precursor solutions were airbrushed onto the Ti support (for prototypes 1 and 2). The procedure was as follows: the material was thermally treated at 130 °C for 30 min to eliminate water, 250ºC for 10 min and, then, at 400°C for 5 min to eliminate the organic materials, which led to the formation of the metallic film. This procedure was repeated five times and, at the end, the Pt loading for each electrode produced was 0.65 mg cm^{-2}. Finally, the electrodes were cooled until room temperature. For the cell in which the MEA is used (prototypes 3 and 4), anodes were prepared as described elsewhere (Lobato et al., 2010) using commercial Pt/C Vulcan (40 %Pt on carbon black, ETech inc) sprayed on a carbon

186 paper (as electrode support, whose geometrical area is 2 cm^2) till obtain the same amount
187 of Pt as in the other anode electrodes, 0.65 mg Pt cm^{-2}.
188 **Cell prototypes.** The goal of this work has been to compare the performance of four types
189 of fuel cells in the production of electricity from chlorine and hydrogen. The four cells
190 use the same membranes, Nafion 117, and the same electrodes: $Ru_{30}Pt_{10}Ti_{60}$ as cathode
191 and a coating of 0.65 mg/cm^2 Pt deposited on Ti ($Pt_{20}Ti_{80}$) or on Vulcan carbon, as anode.
192 Prototypes 1 & 2 used the membrane not only to allow the exchange of the protons
193 through it, but also to separate the anodic compartment from the cathodic one, whereas
194 in the other two cells, prototypes 3 & 4, a MEA was made with the membrane. This
195 membrane, in all the proposed cell prototypes, is continuously hydrated, since this is
196 necessary for the transport of the ionic species through it. The four prototype
197 electrochemical cells proposed were made in-house and each of the two electrodic
198 chambers had a volume of 2 cm^3. Inside these compartments, the electrodes were placed
199 (prototypes 1 and 2) while in the other two cell prototypes, the membrane was sandwiched
200 between the couple of the electrodes, whose dimension is the same as that of these
201 chambers (see Figure SM1 Supplementary Material section).
202 In every case, in the cathode, an aqueous containing hypochlorous acid (1.0M HClO /
203 1.0M HCl) was fed. HCl (37% v/v) was purchased from PanReac (Spain) and HClO (10%
204 v/v) from Sigma-Aldrich (Spain). High solubility of chlorine in water is related to its
205 disproportionation into hypochlorous acid and chloride, which is a very well-known
206 process (eq. 4). For this reason, in this work, direct hypochlorous acid solutions were used
207 instead of absorbing chlorine gas into liquid, in order to reduce the number of inputs to
208 be evaluated in the performance of the different electrochemical cell prototypes tested.
209 $Cl_2 + 2OH^- \rightarrow H_2O + ClO^- + Cl^-$ (4)

Regarding the anode, in three of the four cells (Prototypes 1, 2 and 3), the anolyte consisted of a mixture of hydrogen and a NaCl 2M solution. In fact, it is a biphasic flow with liquid phase of aqueous sodium chloride (2.0 M) mixed with coarse or fine bubbles of H_2(gas), which allows continuous transport of liquid into the cell. To produce coarse bubbles a venturi mixer is used, while to produce fine bubbles a Carmin PMMA D4 Microbubble Generator (YLEC Consultants Fluid Mechanics, France) is included. Flow-dynamics in both cases is going to be very different as it will be discussed in the later Results & Discussion Section.

In the Prototype 4, hydrogen gas is directly fed into the anodic compartment. This gas is distributed homogeneously on the anodic surface of the electrode due to both the configuration of the electrochemical reactor (with an anodic compartment of 2 cm^3) and the size of the electrode used, whose geometrical area is only 2 cm^2, without the need of using a gas diffuser. In every case, the flowrate of hydrogen fed was 0.4 L H_2/minute. Table 1 summarizes the main characteristics of the four cells studied and Figure 1 shows schemes and details to clarify the most important aspects of each prototype.

Table 1. Main features of the four prototypes evaluated in this work

	Cell configuration	**Anodic stream**	**Anolyte**
Prototype 1	Separated membrane & electrodes	Coarse bubbles of H_2 in NaCl 2.0 M aqueous solution	Anodic stream
Prototype 2	Separated membrane & electrodes	Fine bubbles of H_2 in NaCl 2.0 M aqueous solution	Anodic stream
Prototype 3	Membrane-Electrode Assembly	Fine bubbles of H_2 in NaCl 2.0 M aqueous solution	PE Membrane of the MEA + anodic stream
Prototype 4	Membrane-Electrode Assembly	H_2 gas	PE Membrane of the MEA

It is important to highlight that in prototypes 1 and 2, the membrane is only used to separate the anodic and cathodic compartments and it is not in direct contact with the electrodes. Opposite, in prototypes 3 and 4, the membrane is integrated in a MEA made by hot-pressing the membrane in between the cathode and the anode. This whole system was hot-pressed at 120ºC and 1 ton for 5 min (Zamora et al., 2017; Kang et al., 2019). Considering that in all cells the same electrodes are used, differences observed should only be a function of the cell configuration.

Prototypes were connected to electrolyte reservoir tanks (0.1 L) and, during cell operation, both electrolytes were recirculated through the cathodic and anodic compartments using peristaltic pumps (10 L/h), respectively.

Chemical analysis. Chlorine species (Cl^-, ClO^-, ClO_3^-, ClO_4^-) were measured by ion chromatography using Shimadzu LC-20A equipment column, Shodex IC I-524A; mobile phase, 2.5 mM phthalic acid at pH 4; flow rate, 0.5 mL min^{-1}. In the case of hypochlorite, its peak interferes with the chloride ion; for this reason, its determination was carried out by spectrophotometry. The procedure was as follows: 3 mL of the sample were mixed with 50 µL of sodium chloride (3.0 M) and the absorbance of the solution was measured at a wavelength of 293 nm by means of an Agilent 300 Cary series UV–Vis spectrophotometer. The pH was measured with a GLP22 Crison pH meter.

Electrochemical analysis. The electrochemical characterization was performed with an AUTOLAB/PGSTAT 302N potentiostat/galvanostat. All experiments were conducted at atmospheric pressure and room temperature. The cyclic voltammetries were measured in the potential range -1.7 to 1.7V vs SHE, using a sweep rate of 50 mV s^{-1}. The polarization curve was obtained in the potential range 0.0 to 1.4V vs SHE. Potentiometric operation tests (0.5V in fuel cell mode) were carried out to evaluate the performance of each cell.

Results and discussion

Figure 2 shows polarization curves obtained with the four fuel cell prototypes tested in this work. Despite having fed the same reagents, and having used the cells components (membranes and electrodes) in the four cases, the results are completely different and indicates an important influence of the cell configuration on the production of electricity. It is important to take in mind that membrane behaves only as a compartment separator in prototypes 1 and 2, where the distance between the electrodes is rather high (1 cm) and titanium supported anodes are used for chlorine reduction. Differences between these two prototypes rely mainly on the size of the bubbles produced to promote the absorption of the hydrogen gas into the liquid that flows into the cell, carrying the hydrogen.

In the first case, it is coarse bubble (average size 0.88 mm) while in the second, is fine bubble (average size around 90 μm) because of the use of an especial mechanical device that produces a sudden change in pressure, from 3 to 1 bars, favoring the release of these tiny bubbles. Thus, the interfacial surface areas between gas and liquid are very different. With microbubbles, this contact area is much higher, being promoted the dissolution of the gas when it is oxidized on the anode surface. This explains the better performance of Prototype 2, with a maximum power density that it is 80% higher than that of Prototype 1 and which, in addition, can reach much higher operation current densities indicating that mass transfer limitations caused by depletion of hydrogen in the nearness of the anode are much less important. Hence, an efficient gas-liquid absorption process seems to become one the most critical inputs to be considered for the efficient performance of the fuel cell.

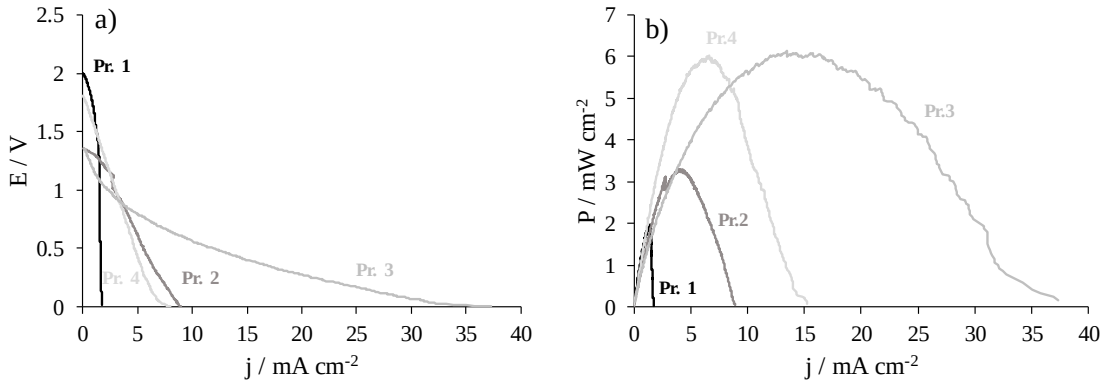

Figure 2. Polarization curves of the four prototypes evaluated in this work: Part a (V vs j); part b (Power vs j). Prototype 1 (-); Prototype 2 (-); Prototype 3(-); Prototype 4 (-)

However, the effect of the bubble size is not only related to the dissolution of hydrogen into the liquid. As commented before, the bubbles size distribution in both systems is rather different. This bubble size distribution was measured using a software for image analysis (Motic Images Plus 3.0). For this, high resolution images (4000x3000) were taken in our system, as can be seen in the Supplementary Material Section (Figure SM2).

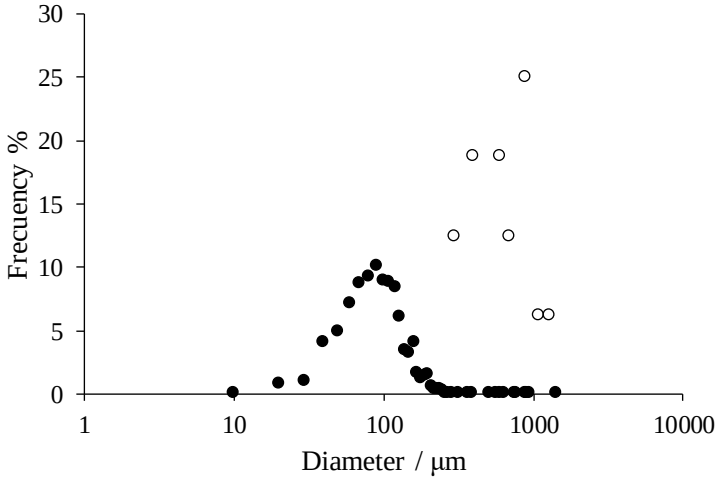

Figure 3. Size distribution curves of hydrogen bubbles. Coarse bubbles (○); Tiny bubbles (●).

Figure 3 shows the distribution is wider in the case of coarse bubbles (0.4-1.4 mm) than in fine bubbles (60-120 µm). This implies that the flow in the pipes and in the anodic

compartment of this biphasic mixture is completely different. For Prototype 1, a slug flow is observed while for Prototype 2 a bubble flow is the primary regime. This helps to explain the important differences observed between these two types of bubbles, as it will be detailed later, because of the influence of this flow on the contact time of reagents with the electrodes.

In the other two prototypes tested in this work, the membrane is integrated into a MEA and, hence, the electrodes are closer to each other. Both the conventional gas based PEMFC (Prototype 4) and the gas-liquid electrochemical cell (Prototype 3) reached similar values of the maximum power density. However, the gas-liquid electrochemical cell has a much lower resistance and it can operate at higher current densities, showing an important advantage in this point.

Comparison of prototypes 3 and 2 is quite interesting. Both systems are fed with tiny bubbles of hydrogen (produced in the mechanical micro-bubble generator), but they have two very different electrodes configuration: Prototype 2 has completely separated the electrodes and the membrane only is used to divide the compartments, while in Prototype 3 there is a real MEA. Anodes have the same Pt loading (0.65 mg/cm^2) although in the prototype 3 it is not dispersed on Ti but on Vulcan carbon in a carbon paper-based electrode, which is expected to be a more efficient distribution. Thus, according to results shown, Prototype 3 compares favorably with Prototype 2, indicating that the proximity of the electrodes, the carbon support, and the simultaneous existence of two electrolytes (media for the transport of ions) become very important points in the design of efficient gas-liquid electrochemical cells to be used in fuel cells applications.

Regarding the cell voltage vs current plot, it is important to highlight the higher OCVs (Open Circuit Voltages) observed for prototypes 1 and 4, in which hydrogen gas is in direct contact with the anode: in the case of the Prototype 4, because only gas is fed to

the cell and no liquid is used as carrier; in the case of Prototype 1, because the coarse bubbling makes that the liquid electrolyte only drags coarse bubbles of hydrogen (slug flow) and hence, what it is really in contact with the electrodes is a gas. On the contrary, in using the mechanical device to produce tiny bubbles, the OCVs are nearly the same in the two cells (despite the very different disposition of the reactors), indicating that, in this case, the reactive species is dissolved hydrogen and not gaseous hydrogen, which is an indicative of the influence of the fuel feeding. In the cathodic zone, the same electrolyte is added, and the same catalyst is used, so differences in the OCV are not expected to be related with this part of the cell, in which the reduction of hypochlorous acid takes place. Likewise, although in prototypes 1&2 and in 3&4 different anode supports are used, the platinum load is the same, so initially not important differences are expected in this point because they are using the same electrocatalyst.

Regarding the shape of the I/V curves, a very important effect of the mass transport limitations can be seen in Prototype 1, which can be related with the slug flow of gas in the anodic chamber, as it is indicated in Table 2, where the fitting parameters of the polarization curves to the model shown in Eq. 5 and developed by Kim et al [39] are indicated, together with the correlation coefficient of the model with respect to the experimental data. In this equation, parameter E_0 is the constant cell voltage fitting parameter, $b\ log(i)$ represents activation losses, $R{\cdot}i$ stands for the ohmic losses, and $m{\cdot}exp(ni)$ is an empirical term that approximates mass transfer loss.

$$E_{cell} = E_0 - b \cdot \log(i) - R \cdot i - m \cdot \exp\,(ni) \qquad [5]$$

Table 2. Fitting of the polarization curves to the model of Kim

Prototype	E_O (V)	b (V/decades)	R (Ω)	m (V)	n (mA^{-} cm^2)	r^2
1	1.79	0.06	0.001	0.01	3.0	0.944
2	1.10	0.30	0.001	0.01	0.5	0.797
3	1.10	0.30	0.02	0.0	0.0	0.984
4	1.79	0.06	0.26	0.0	0.0	0.998

Thus, mass transfer limitations explain the higher value of the slope in the plot of Prototype 1 and the fact that the maximum current density that can be reached is very low. This problem is solved when using a fine bubble producing device, leading to a more efficient distribution of the gas into the liquid, providing reagent once it is exhausted from the liquid and allowing to reach higher current densities. Finally, in comparing prototypes 3 and 4, the double electrolyte in Prototype 3 allows a lower resistance and, hence, to reach much higher operational current densities as compared with the single solid electrolyte used in Prototype 4.

It is also important to mention how the open circuit voltage values (Figure 2) are far from what it could be expected, a phenomenon which may be influenced by several factors including the occurrence of other reactions on the anodic surface such as oxidation of sodium chloride to chlorine and its disproportionation to chlorates, which will be discussed with more detail in Figure 8.

Going deeper inside mass transport, it is important to state that there are important differences in mass transfer coefficients among the different prototypes, as it is indicated

in Figure 4, where it is shown the limiting current density obtained for the actual operation conditions of the cells with a ferro/ferricyanide redox *system* following the procedure describe elsewhere (Canizares et al., 2006) and where it can be seen plateau zones near 20 mA cm^{-2} for prototypes 3 and 4 and 50 mA cm^{-2} for prototypes 1 and 2. From these values, the mass transport coefficients (k) were calculated using Eq. 6, where I_{lim} (A) is the limiting current, whose value is determined from the graph, n is number of exchanged electrons, F is the Faraday constant, A (m^2) represents the electrode surface and C_B ($kmol/m^3$) is the concentration in the bulk solution.

$$k = \frac{I_{lim}}{n \cdot F \cdot A \cdot C_B} \qquad [6]$$

Mass transfer coefficients are more than two times higher in the case of the prototypes where the MEAs are used (prototypes 3 and 4) as compared with those in which the membrane is used only as a compartment separator (prototypes 1 and 2).

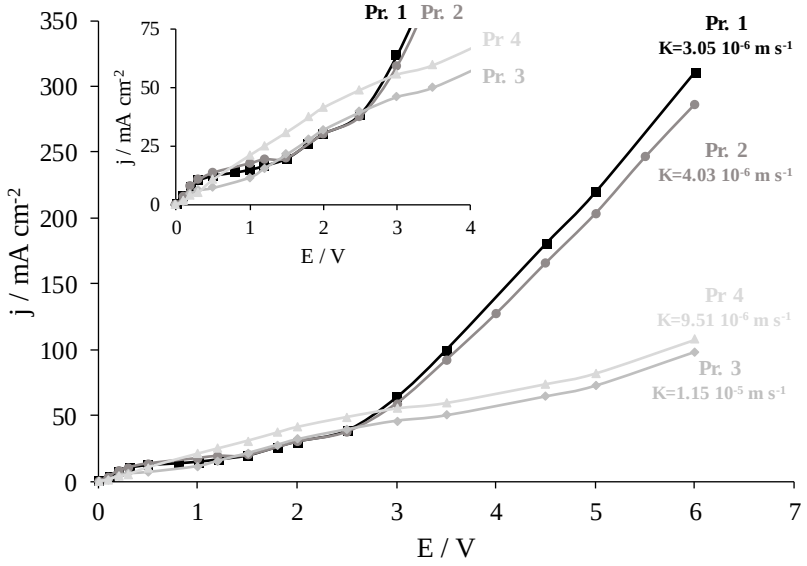

Figure 4. Determination of mass transport coefficients. Current density vs cell voltage curves obtained using ferro/ferricyanide couple (0.5M) (inset figure showing the zoomed view of these curves): Prototype 1 (■); Prototype 2 (●); Prototype 3(♦); Prototype 4 using

371 coarse bubbles instead of direct gas (▲). Calculated values of the mass transfer
372 coefficients.
373
374 In the limiting current plot, it is important to point out two observations:
375 • in the case of cells equipped with MEA, tiny bubbles improve the turbulence and
376 hence the mass transfer coefficient, while in the other cells difference is almost
377 nil (in fact, fine microbubbles produce a slightly better response). Thus, the
378 increase in the mass transfer coefficient when using tiny bubble is nearly 20.7 %
379 when using the MEA, while in the case of the cells with membrane as separator
380 the difference is negligible (below 1.5%);
381 • although not related to mass transport but to side reaction kinetics, behavior of the
382 cells at large cell potentials is completely different, being more important the
383 oxidation of the solvent (water) in case of prototypes 1 and 2. In addition, the
384 limiting current is obtained at lower cells voltages for these cells indicating that
385 ohmic resistances in this type of cells are lower. Therefore, in view of the limiting
386 current density values obtained (19.46 mA cm^{-2} for prototype 1, 19.75 mA cm^{-2}
387 for prototype 2, 45.87 mA cm^{-2} for prototype 3 and 55.37 mA cm^{-2} for prototype
388 4), cell prototypes where MEA is used respond better at the same operation
389 conditions.
390
391 Contact times between electrodes and electrolyte are very important and they can be
392 estimated using the residence time distribution (RTD) plots obtained by a classical
393 procedure applied in the characterization of electrochemical cells (Canizares et al., 2005).
394 They are shown in Figure 5, where it can be seen that the cells equipped with the MEA

(part b) leads to more prolonged contacts times between electrolyte and electrodes than that in which the membrane is not in contact with the electrodes.

For both types of cell prototypes, when hydrogen is introduced, contact time decreases and use of coarse bubbles leads to the occurrence of higher concentrations of tracer in the reactor for shorter times than fine bubbles. In turn, these prototypes exhibit a shorter contact time that the systems without gas addition.

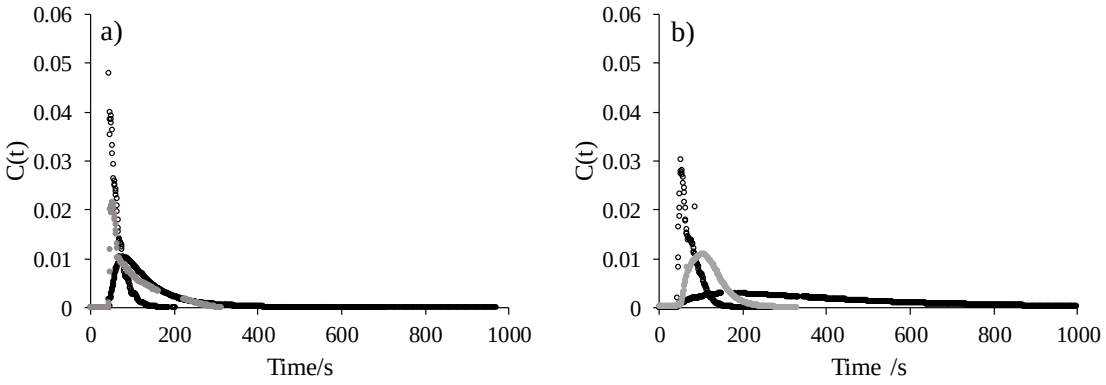

Figure 5. Flow dynamic characterization of the prototypes evaluated in this work. A) cells in which membrane performs as a separator. B) cells equipped with MEA. No hydrogen (●), coarse bubbles (○); tiny bubbles (●)

Part A of Figure 6 shows the operation current density produced by the four fuel cell prototypes operating at a constant cell voltage of 0.5V for 36 minutes (both parameters selected arbitrarily). This test was made for the sake of performance comparison in normal operation. Results are as expected according to the polarization curves. However, there is a rapid decrease in the current exerted by Prototype 3, at the beginning of the process. Then, it increases progressively from 6.5 to 8.2 mA cm^{-2}. In the conventional PEMFC (Prototype 4), except for a small period in which a positive step is observed, the current produced is lower (around 4.8 mA cm^{-2}). Regarding the prototypes 1 and 2, the current produced is much lower, being higher in the case of the system fed with fine

bubbles, as expected. In these tests, it is important to point out the stability of the response of the cell in operation and its fast steadying. This operation results confirm that feeding a biphasic mixture with tiny microbubbles is a good strategy for using gas-liquid reactors as fuel cells.

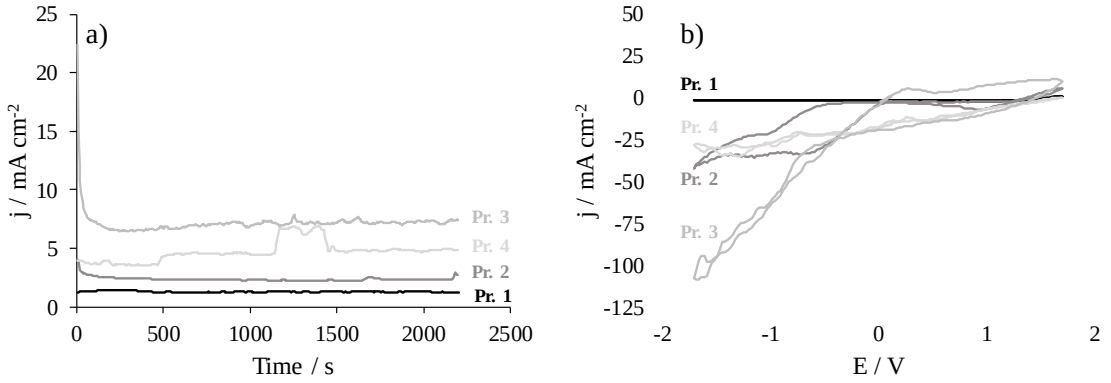

Figure 6. a) Current densities produced during the operation of the four prototypes fed with 0.4 L min^{-1} of hydrogen. b) Cyclic voltammograms obtained directly after the operation tests. Prototype 1 (-); Prototype 2 (-); Prototype 3(-); Prototype 4 (-)

This explanation is supported in Part b of Figure 6, where cyclic voltammograms performed directly in the prototypes are shown, using the Pt anode also as the reference electrode. It can be seen that the response in the region 0 - 1 V vs SHE (where the fuel cell behavior is observed) is much better for cells equipped with the MEA, being higher the achieved current densities in the case of the system fed with tiny bubbles. It can also be observed the same sequence observed in the potentiostatic tests and in the polarization curves. In addition, it is also worth to mention the differences observed in the region of electrolyte decomposition, in particular in the case of the prototypes 3 and 1, which again show the limit behaviors. Therefore, anodic zone highlights the complex influence on

reactivity when feeding liquid electrolyte with coarse or tiny bubbles of hydrogen to the cell.

Figure 7 shows the amount of oxidant consumed during the tests (in the form of hypochlorous acid) in the four fuel cell prototypes, as well as the rate of consumption of hydrogen during this time.

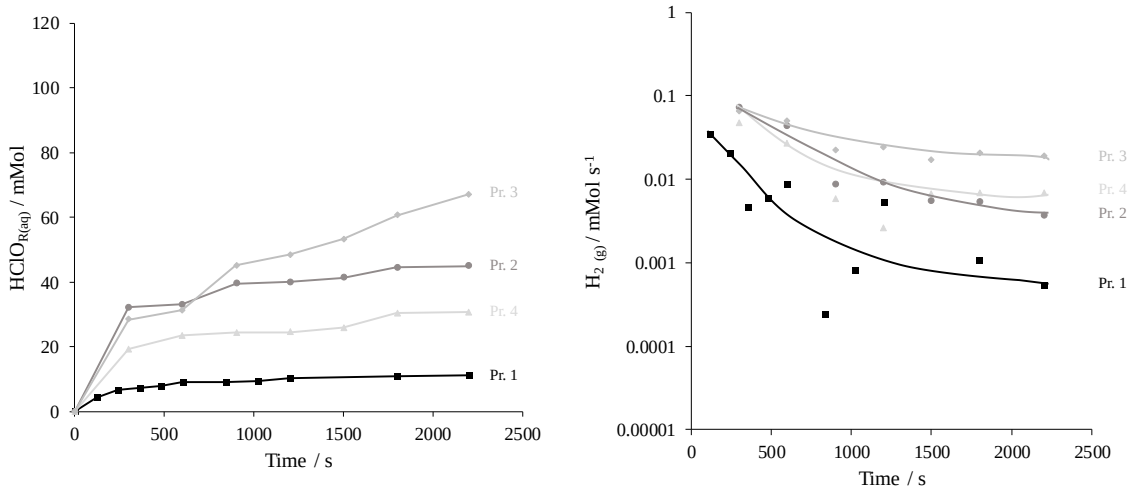

Figure 7. Chlorine consumed (left) and rate of hydrogen consumption (right) during operation in fuel cell mode at 0.5 V. Prototype 1 ■ ; Prototype 2 ●; Prototype 3 ◆, Prototype 4 ▲

As the oxidant fed is the same in the four cell prototypes (a solution of hypochlorous acid/sodium hypochlorite 1.0 M at pH 5), the differences observed indicate that the harnessing is not the same, being more important in the prototypes fed in the anode compartment with microbubbles of hydrogen, in particular in the cell equipped with MEA. This is reflected on the hydrogen consumption rate, which is almost stochiometrically related with the chloride decrease, except for the occurrence of several parasitic reactions, which consists of the formation of chlorine by oxidation of the sodium chloride and the disproportionation of this chlorine to chlorates (Figure 8). Obviously,

these reactions do not occur in the cell fed with gaseous hydrogen, because in that case there is no liquid carrier but only the gas used as fuel flows throughout the compartment.

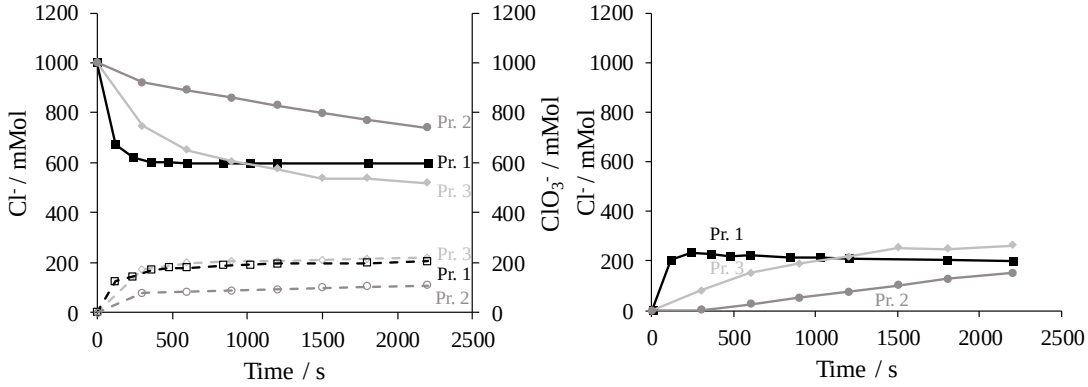

Figure 8. Speciation of chlorine in the anodic chamber of prototypes 1 (■), 2 (●) and 3 (◆). Full points: chloride. Empty points: chlorates

The changes in the rate of hydrogen consumption (and hence in hypochlorite) can be associated to the cathodic process. For the comparison, and in order to extract only comparative information of the anodic reaction, hypochlorite was fed in discontinuous mode, being partially exhausted during the process. This means that it becomes the limiting reagent, and this explains the decrease in the consumption of hydrogen with time. Finally, Figure 9 compares for the four prototypes tested: (1) the average power density obtained at 0.5 V, (2) the efficiency in the use of hydrogen in terms of mWh/mol H_2 according to these tests and (3) the maximum power density according to the polarization curve. Power densities range between 1.9 and 6.1 mW cm^{-2}, being more than 3 times higher in the case of the Prototype 3 as compared with the Prototype 1. These values are low but it has to be taken into account that they have been obtained at room temperature. It is also important to state that power densities obtained by the the fuel cell Prototype 3 are higher than those obtained by the Prototype 4 in which the cell was fed directly with

hydrogen. This confirms that the first approach to electro-absorption cell is a suitable alternative and that cell design has an outstanding influence on results.

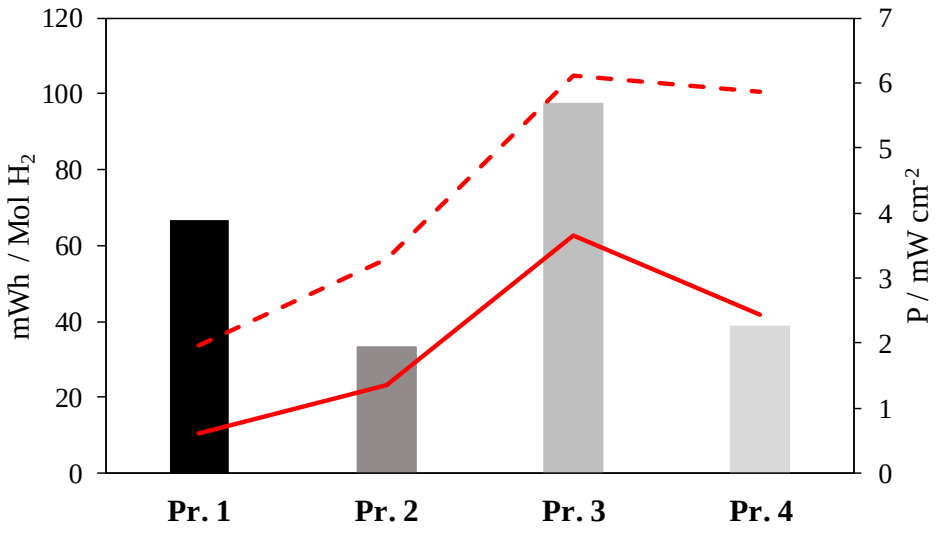

Figure 9. Efficiency in the use of hydrogen (columns) and power density obtained: Dashed line: in the polarization curve. Continuous line: in the test at 0.5V

On the other hand, the efficiency in the use of hydrogen ranges between 33.1 - 97.4 mWh/mol H_2. Again, the cell prototype equipped with the MEA and fed with tiny bubbles attains the higher efficiency in the use of hydrogen. In this case, the second more efficient is Prototype 1, although in this case, the better result can be explained in terms of the lower progress of the reaction and, also, because of the higher concentration of fuel on the electrode surface observed in the RTD curves.

Conclusions

From this work, the following conclusions can be drawn:

- H_2/Cl_2 (chloralkaline) fuel cells can be operated at room temperature with different types of cell prototypes. Gas-liquid electrochemical cells are a suitable

choice for this process, being able to outperform conventional fuel cells fed with hydrogen gas.

- Important differences in the results reached by each type of chloralkaline fuel cell prototype are obtained. Cells equipped with membrane-electrode assemblies are more efficient in the production of electricity than those in which the membrane is only used to separate the electrodic compartments.
- Important differences are obtained between feeding the fuel cells with hydrogen gas or with a biphasic mixture of hydrogen and NaCl electrolyte. In turn, also important differences between mixing coarse or tiny bubbles of hydrogen in the liquid electrolyte fed to the gas-liquid fuel cell. The most efficient performance is attained by the system fed with hydrogen fine bubbles.
- Mass transport is promoted in conventional two-compartment cells (prototypes 1&2) as compared with MEA-equipped cells (prototypes 3&4). Electrolyte-electrode contact time decreases with the bubbling of hydrogen. Coarse bubbles lead to lower contact time but with higher concentrations of fuel in the anodic compartment.
- Even working at low temperatures, significant amounts of electricity are produced. Thus, maximum power reached has been 6.1 mW cm^{-2} with a specific power generated of around 50 mWh g^{-1} hydrogen (Fuel cell prototype 3).

Acknowledgements

Financial support from the Spanish Agencia Estatal de Investigación and European Union through project CTQ2017-91190-EXP (AEI/FEDER, UE) and excellence network CTQ2017-90659-REDT (AEI/FEDER, UE) is gratefully acknowledged. This work also

contains first results of the Project PID2019-107271RB-I00, continuation of the CTQ2017-91190-EXP

Literature cited

Adam Gopal, R., Govindan, M., Moon, I.S., 2018. Enhanced electro-reduction of NO to NH3 on Pt cathode at electro-scrubber. Environmental science and pollution research international.

Balaji, S., Muthuraman, G., Moon, I.S., 2015. Influence of cathode on the electro-generation of peroxydisulfuric acid oxidant and its application for effective removal of SO2 by room temperature electro-scrubbing process. Journal of Hazardous Materials 299, 437-443.

Bebelis, S., Bouzek, K., Cornell, A., Ferreira, M.G.S., Kelsall, G.H., Lapicque, F., de Leon, C.P., Rodrigo, M.A., Walsh, F.C., 2013. Highlights during the development of electrochemical engineering. Chemical Engineering Research & Design 91, 1998-2020.

Bechtel, S., Vidakovic-Koch, T., Sundmacher, K., 2018. Novel process for the exergetically efficient recycling of chlorine by gas phase electrolysis of hydrogen chloride. Chemical Engineering Journal 346, 535-548.

Canizares, P., Carmona, M., Lobato, J., Martinez, F., Rodrigo, M., 2005. Electrodissolution of aluminum electrodes in electrocoagulation processes. Industrial & Engineering Chemistry Research 44, 4178-4185.

Canizares, P., Garcia-Gomez, J., Fernandez de Marcos, I., Rodrigo, M.A., Lobato, J., 2006. Measurement of mass-transfer coefficients by an electrochemical technique. Journal of Chemical Education 83, 1204-1207.

Fernando Perez, J., Llanos, J., Saez, C., Lopez, C., Canzares, P., Andres Rodrigo, M., 2019. Towards the scale up of a pressurized-jet microfluidic flow-through reactor for cost-effective electro-generation of H2O2. Journal of Cleaner Production 211, 1259-1267.

Freitas, R.G., Oliveira, R.T.S., Santos, M.C., Bulhoes, L.O.S., Pereira, E.C., 2006a. Preparation of Pt thin film electrodes using the Pechini method. Materials Letters 60, 1906-1910.

Freitas, R.G., Santos, M.C., Oliveira, R.T.S., Bulhoes, L.O.S., Pereira, E.C., 2006b. Methanol and ethanol electroxidation using Pt electrodes prepared by the polymeric precursor method. Journal of Power Sources 158, 164-168.

Govindan, M., Moon, I.-S., 2015. Uncovering results in electro-scrubbing process toward green methodology during environmental air pollutants removal. Process Safety and Environmental Protection 93, 227-232.

Kang, Y.S., Jo, S., Choi, D., Kim, J.Y., Park, T., Yoo, S.J., 2019. Pt-Sputtered Ti Mesh Electrode for Polymer Electrolyte Membrane Fuel Cells. International Journal of Precision Engineering and Manufacturing-Green Technology 6, 271-279.

Lobato, J., Canizares, P., Rodrigo, M.A., Linares, J.J., Aguilar, J.A., 2007. Improved polybenzimidazole films for H3PO4-doped PBI-based high temperature PEMFC. Journal of Membrane Science 306, 47-55.

Lobato, J., Canizares, P., Rodrigo, M.A., Linares, J.J., Javier Pinar, F., 2010. Study of the influence of the amount of PBI-H3PO4 in the catalytic layer of a high temperature PEMFC. International Journal of Hydrogen Energy 35, 1347-1355.

Perez, J.F., Llanos, J., Saez, C., Lopez, C., Canizares, P., Rodrigo, M.A., 2019. On the design of a jet-aerated microfluidic flow-through reactor for wastewater treatment by electro-Fenton. Separation and Purification Technology 208, 123-129.

Pillai, K.C., Chung, S.J., Raju, T., Moon, I.-S., 2009. Experimental aspects of combined NOx and SO2 removal from flue-gas mixture in an integrated wet scrubber-electrochemical cell system. Chemosphere 76, 657-664.
Thomassen, M., Borresen, B., Scott, K., Tunold, R., 2006a. A computational simulation of a hydrogen/chlorine single fuel cell. Journal of Power Sources 157, 271-283.
Thomassen, M., Karlsen, C., Borresen, B., Tunold, R., 2006b. Kinetic investigation of the chlorine reduction reaction on electrochemically oxidised ruthenium. Electrochimica Acta 51, 2909-2918.
Thomassen, M., Sandnes, E., Borresen, B., Tunold, R., 2006c. Evaluation of concepts for hydrogen - chlorine fuel cells. Journal of Applied Electrochemistry 36, 813-819.
Verhage, A.J.L., Coolegem, J.F., Mulder, M.J.J., Yildirim, M.H., de Bruijn, F.A., 2013. 30,000 h operation of a 70 kW stationary PEM fuel cell system using hydrogen from a chlorine factory. International Journal of Hydrogen Energy 38, 4714-4724.
Yang, J., Liu, K., Jia, J., Cao, L., 2011. Electro-scrubbing volatile organic carbons in the air stream with a gas diffusion electrode. Journal of Hazardous Materials 188, 125-131.
Zamora, H., Plaza, J., Canizares, P., Rodrigo, M.A., Lobato, J., 2017. High-Stability Electrodes for High-Temperature Proton Exchange Membrane Fuel Cells by Using Advanced Nanocarbonaceous Materials. Chemelectrochem 4, 3288-3295.